Stem Cell Reports
Report
ISSCR
OPEN ACCESS

SOX2 Is a Marker for Stem-like Tumor Cells in Bladder Cancer

Fengyu Zhu,[1,3] Weiqing Qian,[2,3] Haojie Zhang,[2,3] Yu Liang,[1] Mingqing Wu,[1] Yingyin Zhang,[1] Xiuhong Zhang,[1] Qian Gao,[1] and Yang Li[1,*]
[1]Department of Biology, School of Life Science, Anhui Medical University, Hefei, Anhui 230031, China
[2]Department of Urology, Huadong Hospital, Fudan University, Shanghai 200040, China
[3]Co-first author
*Correspondence: liyang@ahmu.edu.cn
http://dx.doi.org/10.1016/j.stemcr.2017.07.004

SUMMARY

It has been reported that functionally distinct cancer stem cells (CSCs) exist in human bladder cancer (BCa). Here, we found that *Sox2*, a transcription factor that is well characterized as a marker for stem cells, is upregulated in both mouse and human BCa. *Sox2* expression is absent in normal urothelial cells, but it begins to be expressed in pre-neoplastic bladder tumors and continues to be expressed in invasive mouse BCa. Using s as a reporter of *Sox2* transcriptional expression, we demonstrated that *Sox2*-expressing cells mark a subpopulation of tumor cells that fuel the growth of established BCa. SOX2-positive cells also expressed other previously reported BCa CSC markers, including Keratin14 (KRT14) and CD44v6. Ablation of *Sox2*-expressing cells within primary invasive BCa led to enhanced tumor regression, supporting the essential role of SOX2-positive cells in regulating BCa maintenance and progression. Our data show that *Sox2* is a marker of bladder CSCs and indicate it as a potential clinical target for BCa therapy.

INTRODUCTION

Bladder cancer (BCa) is the sixth most common malignancy in males worldwide, affecting ~429,800 people annually and is responsible for ~165,100 deaths (Torre et al., 2015). Treatment with chemotherapeutics or surgical resection for BCa usually fails due to the existence of cancer stem cells (CSCs). CSCs play a pivotal role in tumor recurrence and metastasis and make complete elimination of the tumor difficult. The ability of these bladder CSCs to drive cancer initiation and progression make them ideal targets for anticancer therapies. Improvement in clinical treatment strategies requires further understanding of the CSC population and their molecular biology.

Research on the phenotypic and functional properties of urothelial CSCs has revealed that they are not characterized by a one-marker-fits-all approach; instead, various markers, including the aldehyde dehydrogenase 1 family, member A1 (*ALDH1A1*), cytokeratin 14 (*CK14*), and *CD44v6*, are used to isolate CSCs from patient specimens and to successfully establish cancer cell lines (Chan et al., 2010; Ho et al., 2012a). These CSCs appear to differ considerably and may contribute to the heterogeneity of BCa (Hatina and Schulz, 2012).

The transcription factor SOX2 is a member of the SRY-related HMG-box (SOX) family. It plays an essential role in cell fate determination, thereby regulating developmental processes (Sarkar and Hochedlinger, 2013). Aberrant expression of *SOX2* has been reported in many types of cancers and is correlated with the presence of CSCs (Ferone et al., 2016; Leis et al., 2012; Lundberg et al., 2016). As for BCa, *SOX2* expression is associated with tumor progression and prognosis (Kitamura et al., 2013; Ruan et al., 2013). Nevertheless, *SOX2*-expressing cells have yet to be identified in the normal human urothelium, and definitive proof that SOX2-positive cells correspond to urothelial malignancies remains elusive.

Here, we provide unequivocal evidence that the expression of *Sox2* is rare in the normal bladder epithelia but remarkably elevated in BCa of both mouse and human patient origin. SOX2+ cells isolated from BCa tissue had a much greater ability to reform secondary tumors *in vivo* and spheres *in vitro* compared with SOX2 cells. Lineage-tracing experiments showed that SOX2+ cells give rise to a spectrum of bladder tumors. SOX2+ cells are highly coincident with KRT14- and CD44v6-positive urothelial CSCs. Furthermore, ablation of SOX2+ cells in BCa by administration of tamoxifen to *Sox2*^{CreER}*:Rosa-DTA* mice led to a strong regression of invasive BCa. These findings suggest that SOX2 marks a population of tumor cells necessary for tumor growth and maintenance *in vivo* and will inspire future studies regarding their role in bladder tumorigenesis and their use in medicine applications.

RESULTS

Sox2 Expression Is Elevated in BCa Tissue

To gain insight into the role of *Sox2* in BCa progression *in vivo*, we examined its expression in samples from a cohort of 22 BCa patients by immunohistochemistry (n = 22) and found *Sox2* expression was significantly higher than in the para-tumor samples (n = 7; Figures 1A and 1C). We further crossed *Sox2*^{CreER} mice with *R26*^{tdTomato} mice and made use of an N-butyl-N-4-hydroxybutyl nitrosamine (BBN)-induced bladder carcinogenesis mouse model that

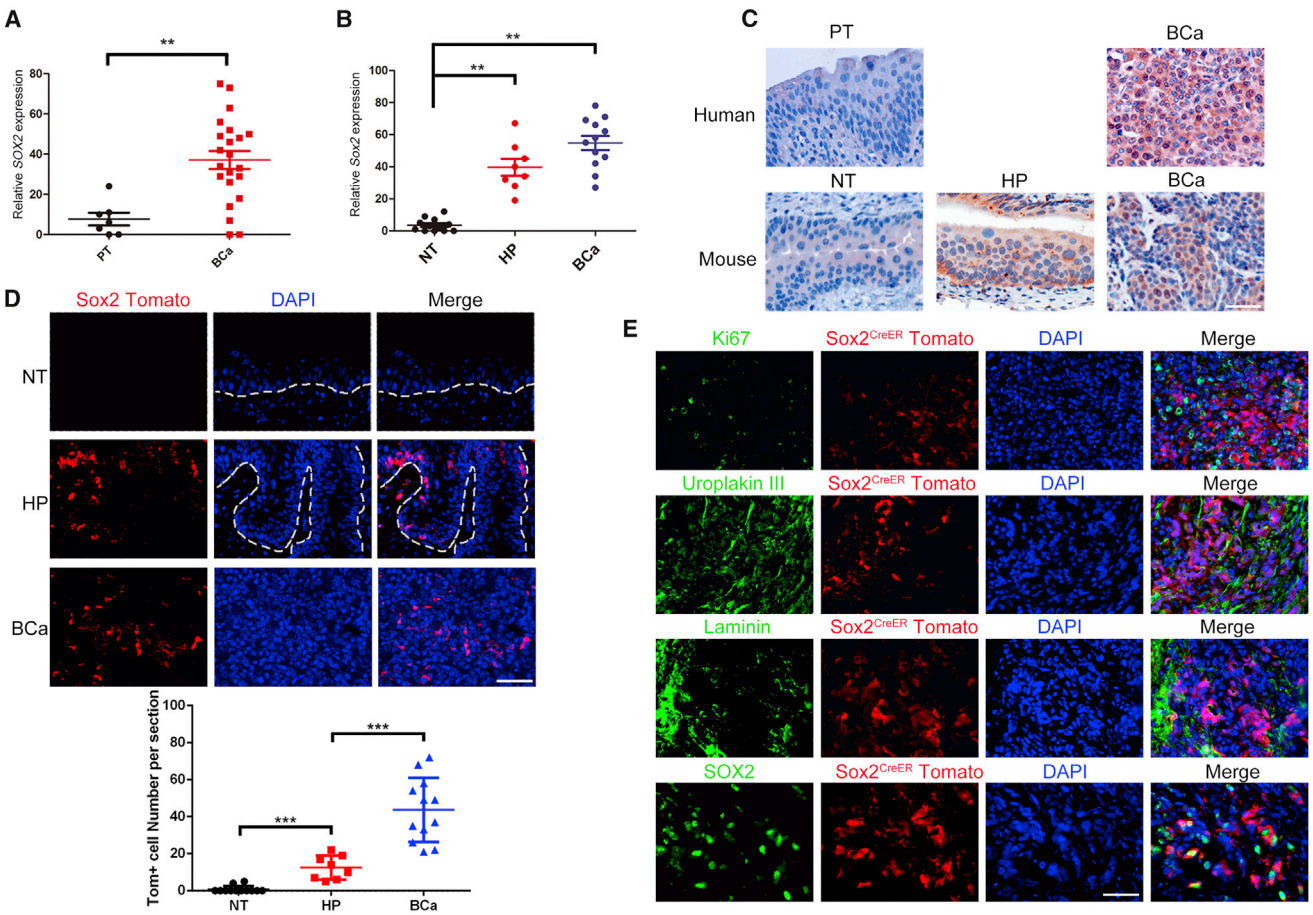

Figure 1. *Sox2* Expression in Normal Bladder Tissue and BCa Samples

(A and B) Quantitative measurement of SOX2 in (A) human and (B) mice bladder tumor tissues (BCa, n = 22 for human samples, and n = 12 for mice samples), hyperplasia tissue (HP, n = 8), and normal tissues (NT, n = 12)/para-tumor tissue (PT, n = 7). The intensities of immunostaining were quantitatively measured using Image-Pro Plus 6.0 image analysis software. **p < 0.01, Student's t test and one-way ANOVA.

(C) Representative image of immunohistochemical staining by SOX2 antibody in both human and mouse BCa samples and hyperplasia tissue (HP) compared with human para-tumor tissue (PT) and mouse normal bladder tissues (NT).

(D) Permanent labeling of SOX2+ cells by activation of a *tdTomato* transgene in samples from *SOX2*^{CreER};*R26*^{tdTomato} mouse with tamoxifen injection at different stages of tumor progression (same sample numbers used as in B). ***p < 0.001 by one-way ANOVA; dashed lines represent the basement membrane.

(E) Representative sections from the mouse BCa samples were stained by the indicated antibodies.

Scale bars, 50 μm.

shares molecular similarities with the human disease (Williams et al., 2008). Specifically, urothelial hyperplasia in mice (n = 8) was induced by administration of BBN for 14 weeks, whereas invasive BCa in mice (n = 12) was induced by administration of BBN for 26 weeks. We found that the expression of *Sox2* in mice with urothelial hyperplasia and mice with invasive BCa was elevated compared with normal bladder tissue. In fact, *Sox2* expression was hardly detected in the normal bladder tissue in mice but began to be broadly observed in hyperplasia tissue and BCa samples, ranging from several scattered cells to aggregated clusters (Figures 1B and 1C). When tamoxifen was applied to these tumor-bearing *Sox2*^{CreER}:*R26*^{tdTomato} mice as well as the non-treatment normal control mice, we found *Sox2-tdTomato* expression was absent in bladder sections from normal mice. In contrast, we began to observe Sox2-tdTomato in hyperplasia tissue and this was readily observed in BCa samples 3 days after tamoxifen injection (Figure 1D). Immunofluorescent staining with specific antibodies for SOX2 showed a *bona fide Sox2* expression indicated by Tomato fluorescence. Moreover, Ki67 (a proliferation indicator) and Uroplakin III (a differentiation

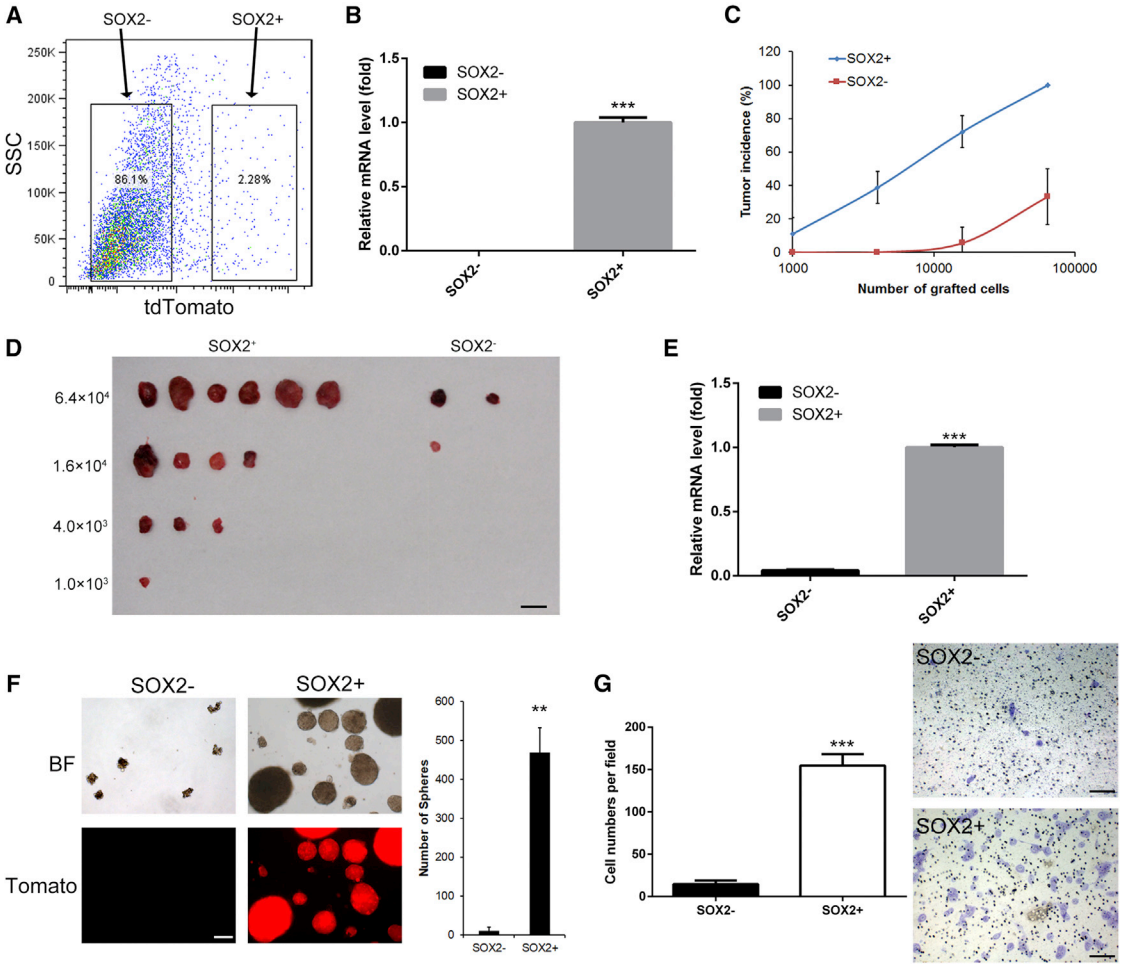

Figure 2. SOX2 Marks BCa-Tumor-Propagating Cells

(A) Representative gating scheme with typical tomato+ and tomato− frequencies for FACS of a BCa tissue from *Sox2*^{CreER};*R26*^{tdTomato} mice.

(B) mRNA levels of *Sox2* were examined by qPCR in sorted Tom+/− cells, respectively.

(C and D) Percentage of tumor-free mice 5 weeks after subcutaneous injection of different dilutions of SOX2-positive or -negative cells into immunodeficient mice in triplicate experiments. In each replicate, 6 mice were used per dilution per condition (SOX2+, SOX2-). Image of a tumor from one dilution assay is shown in (D). Scale bars, 10 mm.

(E) mRNA levels of *Sox2* were examined by qPCR from the tumor samples generated by SOX2+/− cells, respectively.

(F) Tomato-negative (SOX2−) and Tomato-positive (SOX2+) cells were FACS sorted and cultured in stem cell medium. Cultures at 10 days are shown, and the sphere numbers are plotted. BF, bright field. Scale bars, 250 μm.

(G) Matrigel invasion assays were performed with SOX2+/− cells (36 hr) to examine the effects of *Sox2* expression on tumor cell invasion. Scale bars, 50 μm.

**p < 0.01, ***p < 0.001, t test. All error bars represent the SD of three independent experiments.

indicator) staining showed that SOX2+ cells (Tomato+) do not overlap with Ki67- and Uroplakin III-expressing cells, suggesting that SOX2+ cells in BCa may be quiescent and stem cell-like (Figure 1E).

Sox2 Expression Marks a Tumor-Propagating Population of BCa

The current gold standard assay to evaluate CSC potential is to transplant highly purified and properly identified cancer cell populations in a limiting dilution fashion into immune-deficient mice to assess their ability to form secondary tumors (Beck and Blanpain, 2013). To investigate the tumorigenicity of SOX2+ cells in BCa, Sox2+ (Tomato+) and SOX2- (Tomato−) cells were isolated from mice with invasive BCa samples by flow cytometry (Figure 2A). The percentage of viable cells was examined using trypan blue staining for each group to exclude the effect of possible differences in cell viability after cell sorting on the following

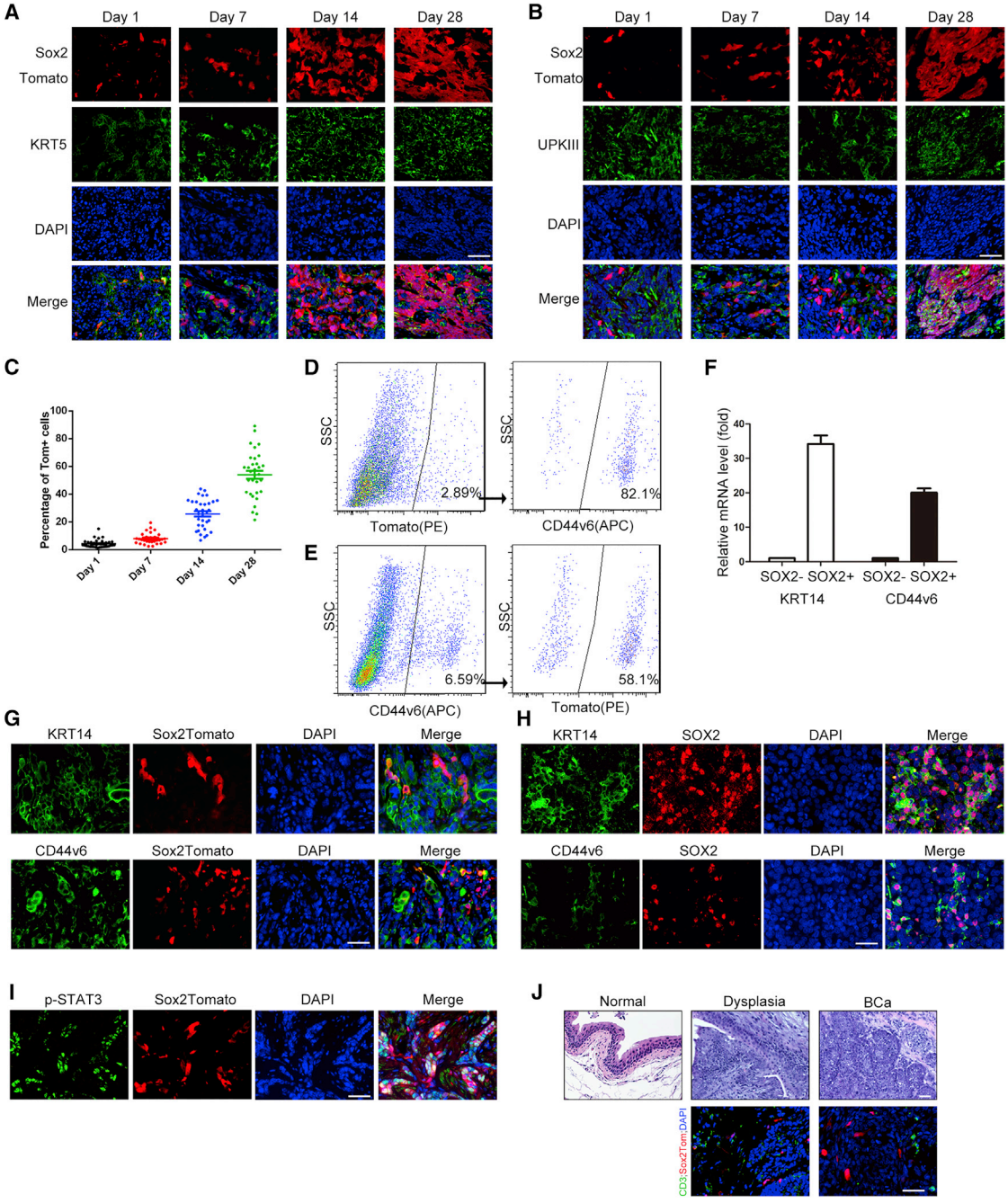

Figure 3. SOX2+ Cells Are the Cells of Origin of BCa

(A and B) Representative images of tdTomato-labeled SOX2+, and Laminin (A) or Uroplakin III (B) stained cells at 1, 7, 14, and 21 days of tracing.

(C) Percentage of the Tom+ cells in the tumor area at each time point after tamoxifen injection, 12 fields for each mouse (3 mice per time point) were selected for calculation.

(D and E) Representative gating scheme with typical Tomato+ (PE) and CD44v6+ (APC) frequencies for FACS of BCa tissue from *Sox2*^{CreER};*R26*^{tdTomato} mice.

(F–H) Relative mRNA level of *Krt14* and *CD44v6* of SOX2+/− cells isolated from BCa tissue from *Sox2*^{CreER};*R26*^{tdTomato} mice. Error bars represent the SD of three independent experiments. Immunofluorescent staining on invasive BCa sections from mouse (G) and human patient samples (H), showing the SOX2+ cell population and extensive co-localization with KRT14 or CD44v6.

(legend continued on next page)

assays (Figure S1). *Sox2* mRNA level in sorted tomato cells was hardly detected by qPCR (Figure 2B). SOX2+ and SOX2− cells were then injected subcutaneously into immune-deficient mice, and tumor formation was measured over time. SOX2+ cells exhibited a significantly higher tumor-propagating potential than the negative cells comprising the tumor bulk (Figures 2C and 2D). Not surprisingly, the *Sox2* mRNA level was much lower in SOX2− xenograft samples than in SOX2+ xenografts (Figure 2E). In addition, these different populations were also seeded on low-attachment plates in clonogenic densities. After a 2-week culture period, we found that the SOX2+ cells produced many more spheres with ideal spherical shape and sharp edges than the SOX2− cells (Figure 2F, $p < 0.01$). Fluorescence microscopy also confirmed the sphere-forming capacity of SOX2+ cells. Moreover, we also assessed the invasiveness of the two cell types using a transwell chamber assay. The SOX2+ cells had significantly higher invasion potential than SOX2− cells (Figure 2G, $p < 0.001$). These results illustrate the clonogenic potential of SOX2+ cells from BCa *in vivo* and *in vitro*.

Genetic Labeling and Lineage Tracing of SOX2+ Cells in BCa

As shown in Figure 1E, we have generated $Sox2^{CreER}$:$R26^{tdTomato}$ mice, and *CreER* expression is indicated by co-expression of *Sox2* and *Tomato* in BCa samples. In the absence of tamoxifen administration, no labeled cells were observed in any BCa samples from these mice, demonstrating the absence of leakiness in these mice (data not shown). To investigate the role of SOX2+ cells in tumor maintenance and progression, 12 male $Sox2^{CreER}$:$R26^{tdTomato}$ mice were exposed to BBN for 24 weeks, followed by a 4-mg dose of tamoxifen that was administered for 3 consecutive days. The mice were then killed on successive days following the tamoxifen regimen (3 mice per time point). Twenty-four hours after the final tamoxifen injection, Tomato-labeled SOX2+ cells were evident in the BCa tissue, and the frequency of positively labeled cells increased progressively (Figures 3A–3C). Twenty-eight days after the last tamoxifen injection, more than 50% of tumor cells were positive for Tomato, indicating that they were derived from the SOX2+ cells initially marked at the time of the injections (Figures 3A–3C). Immunofluorescent staining confirmed that some of these Tomato+ cells still expressed *Sox2* (Figure S2), which further demonstrated the self-renewal capacity of this population *in vivo*. To determine the relationship with other known CSC markers, we co-stained with another *in vivo* CSC marker of BCa, KRT5 (Van Batavia et al., 2014). At the early stages, co-staining indicated that the SOX2+ cells seemed to arise from these KRT5+ stem cells. The SOX2+ cells then began to proliferate and differentiate until, after 28 days, there were large SOX2+ colonies, of which only some contained KRT5+ cells (Figure 3A). In contrast, the SOX2+ cells were initially negative for Uroplakin III 24 hr after the final tamoxifen injection yet, after 28 days, many of the SOX2+ cells were also positive for Uroplakin III (Figure 3B). These results support the notion that Sox2+ lineages in the BCa are capable of self-renewal and differentiation.

Previous studies have reported that KRT5+, KRT14+, and CD44v6+ cells initiate BCa (Papafotiou et al., 2016; Shin et al., 2014; Van Batavia et al., 2014), and *Krt5* expression absolutely coincided with *Krt14* expression in BBN-induced BCa (Papafotiou et al., 2016). To further investigate the relationship between SOX2+ cells and other reported BCa progenitors, we first analyzed CD44v6 expression in fluorescence-activated cell sorting (FACS)-sorted *Sox2*-Tomato+ cells from BBN-induced BCa tissue and found that more than 90% of SOX2+ cells also expressed high levels of CD44v6 (Figure 3D). The CD44v6+ population of cells was therefore isolated from BCa tissue, and we found that, of those cells, about 60% were also SOX2+ (Figure 3E). In addition, we examined the mRNA levels of *CD44v6* and *Krt14* in both SOX2+/− cell populations. Using flow cytometry, we found that SOX2+ cells have a significantly higher expression of both *CD44v6* and *Krt14* than SOX2− cells (Figure 3F). We then stained the cells with KRT14 and CD44v6 antibodies from BBN-induced BCa samples in mice. Similar to the results of KRT5 staining (Figure 3A), Tomato+ (SOX2+) cells, after 3 days of tamoxifen injection, showed a high concurrence with KRT14- and CD44v6-stained cells. Nearly 100% of SOX2+ cells were also positive for KRT14 and CD44v6, while about 40% of KRT14-stained cells and 50% of CD44v6-stained cells were SOX2 positive (Figure 3G). Double staining of the sections from patient samples with SOX2 and KRT14 or CD44v6 antibodies also showed similar results (Figure 3H). Intriguingly, when a sphere assay was performed using CD44v6+Tomato + or CD44V4+Tomato− cells respectively, both groups had the ability to form spheres *in vitro*, but the CD44v6+Tomato+ group formed a significantly greater number of spheres, which were also significantly larger than the CD44v6+Tomato− group (Figure S3). To explore

(I) Immunofluorescent staining on invasive BCa sections from mouse, showing the SOX2+ cell population and extensive co-localization with phosphorylated STAT3 (p-STAT3).

(J) H&E and immunofluorescent staining of BCa sections from mouse at different stages, showing histological change and infiltrated CD3+ T cells during the tumor development.

Scale bars, 50 μm.

the mechanism of how *Sox2* expression regulated the stemness of BCa stem cells, we further investigated the expression of SOX2 target genes that control tumor proliferation and metabolism and are also associated with stemness in other systems. Specifically, we investigated the expression of the following SOX2 target genes: *Igf2bp2*, *Myef2*, *St6gal1*, *Msi2*, *Hmga2*, *Tp63*, *Ccnd1*, *Ccnd2*, *Ccnd3*, *Cdc25c*, *Tex15*, *Enpp1*, *Rap2b*, *Pcdh18*, *Alcam*, *Epha7*, and *Mgll* (Boumahdi et al., 2014; Hutz et al., 2014; Santini et al., 2014). The mRNA levels of *Myef2*, *St6gal1*, *Tp63*, *Ccnd3*, *Cdc25c*, *Pcdh18*, and *Epha7*, were all elevated in CD44v6+/SOX2+ cells compared with CD44v6+/SOX2− cells (Figure S4), indicating the specificity of the SOX2-regulated genes in BCa stem cells. These data indicate that SOX2+ cells may be a subpopulation of KRT14- or CD44v6-marked CSCs and possibly further enable their stem-like capabilities.

Ho et al. (2012b) have shown that *Stat3* activation in CSCs leads to tumor progression and is colocalized with KRT14 + CSCs in BBN-induced mouse BCa. To investigate the possible mechanism of *Sox2* activation in BCa CSCs, we also stained the cells from BBN-induced BCa in mice. We found that STAT3 signaling was activated in most of the SOX2+ (Tom+) stem cells in the tumor (84.7% ± 9.1%, Figure 3I). STAT3 signaling in CSCs can be activated by chemokines such as interferon (IFN)-γ, interleukin (IL)-6 and IL-22 which are released by infiltrated T cells, other lymphocytes, and tumor cells (Yu et al., 2007). To explore whether extracellular signaling, especially tumor-infiltrated lymphocytes, participate in the activation of *Stat3* activation in SOX2+ CSCs, we then examined the presence of CD3-labeled T cells during BCa tumor development. The results showed that lymphocytes were seldom seen in normal bladder tissue, while CD3+ T cells (and probably other lymphocytes) were extensively infiltrated into the tumor microenvironment throughout tumor progression (Figure 3J).

Ablation of Sox2-Expressing Cells Abrogates BCa Progression

To further investigate the role of SOX2+ cells in BCa, we crossed $Sox2^{CreER}$ mice with a Rosa-DTA strain to evaluate the impact of SOX2+ cell lineage ablation on tumor growth and progression. We first induced BCa in $Sox2^{CreER}$:*Rosa-DTA* mice using BBN administration for 26 weeks. To ablate the SOX2+ cells, we then injected the mice with tamoxifen for 3 consecutive days. Two weeks after the injections, we observed a marked regression in tumor size (n = 4, Figures 4A and 4C), along with a reduction in the KI-67+ cell ratio in the tumor lesion compared with the control group (Figures 4B and 4C). Moreover, while there were still KRT14+ and CD44v6+ cells remaining in the tumor lesion after *Sox2* ablation (Figures 4B and 4C), they were present at a lower percentage than in the control mice. Furthermore, an equal number of cancer cells (1×10^7) from the induced BCa tissues of $Sox2^{CreER}$:$R26^{tdTomato}$ and $Sox2^{CreER}$:*Rosa-DTA* mice were transplanted into immune-deficient mice before treating them with tamoxifen for 3 consecutive days. After 3 weeks, all 8 recipients injected with BCa cells from $Sox2^{CreER}$:$R26^{tdTomato}$ mice formed noticeable tumors (8/8, Figure 4D), while cells from $Sox2^{CreER}$:*Rosa-DTA* mice generated only a single, small tumor in one nude mouse (1/8; Figure 4D). These results confirmed that SOX2 marks a population of tumor cells necessary for tumor growth and maintenance *in vivo*.

DISCUSSION

Because cancers have a high hierarchical organization, mapping the fate of the stem and/or non-stem populations to determine the direction of hierarchies is important for cancer therapeutic implications. Many markers of BCa stem cells *in vivo* have been reported, which include CD44, Cytokeratin 5 (*Krt5*) (Chan et al., 2009; Van Batavia et al., 2014), *Krt14* (Papafotiou et al., 2016), and sonic hedgehog (*Shh*) (Shin et al., 2014), all of which are expressed in the cells that arise from basal urothelium. Our findings suggest SOX2+ CSCs have a high coincidence rate with KRT14 and CD44v6+ cells, which indicates that the SOX2+ population in BCa may also be derived from the basal layer of the urothelium. However, lineage ablation of SOX2+ cells in BCa did not fully eliminate KRT14- and CD44-expressing cells, suggesting that SOX2+ stem cells may be a subpopulation of KRT14+ CSCs. In addition, CD44v6+/SOX2− cells also showed ability to formed spheres *in vitro* (although relative weaker than the SOX2+ cells), indicating it is possible that there are other SOX2− CSCs in BCa, which will require further investigation.

To our knowledge, there is still not any direct evidence to support that *Krt14* and *CD44v6* are regulated by SOX2. However, SOX2+ cells have been identified as CSCs in the Shh+ subgroup of medulloblastoma (Vanner et al., 2014), and SOX2 controls the expression of the *Shh* in postnatal neural stem cells and the developing hippocampus (Favaro et al., 2009). Further, *Sox2* is also reported to be regulated by shh signaling and contributes to the CSCs from non-small-cell lung cancer (Bora-Singhal et al., 2015). Shh signaling is also important in promoting the tumorigenicity and stemness of BCa (Islam et al., 2016). All these reports suggest a close correlation between *Sox2*-expressing cells and shh-expressing cells, and their relationship in the context of BCa stem cells awaits further study.

Our data suggest *Sox2* expression is absent in normal urothelial cells of both human and mouse. Understanding how *Sox2* is expression is activated in CSCs of BCa may be important to interpret the carcinogenesis of BCa *in vivo*.

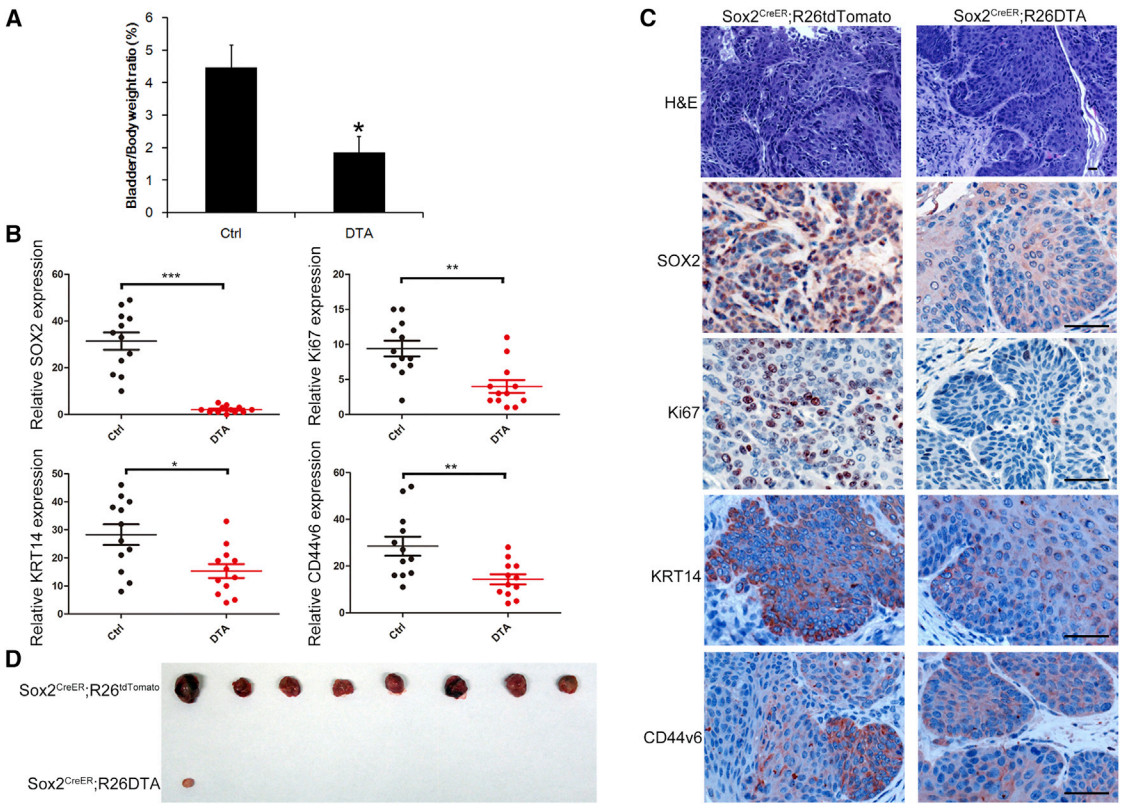

Figure 4. *Sox2* Lineage Ablation Leads to Regression of Pre-existing BCa

(A) The G/B ratio was calculated as (gross bladder weight/body weight) × 100% and analyzed with Student's t test for both groups; n = 4, *p < 0.05.

(B) Quantitative measurement of SOX2, Ki67, KRT14, and CD44v6 expression in bladder tumor tissues (BCa) from $Sox2^{CreER};R26^{tdTomato}$(Ctrl) or $Sox2^{CreER};R26^{DTA}$(DTA) mice. Three different areas from each mouse (4 mice per group) were randomly picked, and the intensity of immunostaining was quantitatively measured using Image-Pro Plus 6.0 image analysis software. *p < 0.05, **p < 0.01, ***p<0.001, Student's t test.

(C) Representative histopathology and immunohistochemical staining of tumor tissues with indicated antibodies are shown.

(D) Tumor image showing secondary recipients 3 weeks after subcutaneous injection of the same number of tumor cells from *Sox2* Tom or *Sox2* DTA mice into immunodeficient mice.

Scale bars, 50 μm.

Genetic amplification of *SOX2* has been reported in some cancers, including SCCs from lung and esophagus (Bass et al., 2009). According to the TCGA Bladder Urothelial Carcinoma (provisional raw data at the NCI), there are 65 BCa patients with amplification of the *SOX2* location (chr3:3q26.33) in a survey of 412 patients (http://cancergenome.nih.gov/). For transcriptional regulation, *SOX2* can be activated by STAT3 in embryonic cells (Foshay and Gallicano, 2008), and it cooperates with STAT3 to initiate malignant transformation in the forestomach (Liu et al., 2013). In BCa, STAT3 signaling is activated in CSCs and leads to BCa progression (Ho et al., 2012b). Our data also suggest a high co-localization of activated STAT3 with SOX2+ cells in BCa. Another possible mechanism of *Sox2* activation is epigenetic regulation; SOX2 can be activated by JMJD2A (Bouzas et al., 2016), which is the demethylase of H3K9me3 and is often highly expressed in BCa (Kogure et al., 2013).

In conclusion, our studies shed light on *Sox2* as a marker for stem-like tumor cells of BCa *in vivo*. How and when *Sox2* expression becomes activated in BCa progression and whether it is involved in cancer cell fate determination will be the subject of future investigation.

EXPERIMENTAL PROCEDURES

All animal procedures were performed under a protocol approved by the Laboratory Animal Center of Anhui Medical University and in accordance with the *NIH Guide for the Care and Use of Laboratory Animals* (NIH Publications No. 8023, revised 1978).

Clinical Sample

Twenty-two human BCa samples were obtained from the Department of Urology, Huadong Hospital, Fudan University, with patients' informed consent. The pathological condition of the BPH samples was determined by experienced urologists at Huadong Hospital. This study was conducted under the approval of Ethics Committee of Huadong Hospital affiliated to Fudan University.

Statistics

Data are presented as the means ± SD or SE. All of the statistical analyses were performed using Excel (Microsoft, Redmond, WA) or Prism (GraphPad Software, La Jolla, CA). The two-tailed Student's t test or one-way ANOVA was used and a p value <0.05 was considered significant.

SUPPLEMENTAL INFORMATION

Supplemental Information includes Supplemental Experimental Procedures and four figures and can be found with this article online at http://dx.doi.org/10.1016/j.stemcr.2017.07.004.

AUTHOR CONTRIBUTIONS

F.Z., Y. Liang, and M.W. did the experiments; H. Z. and W.Q. provided and analyzed the clinical samples; Y. Li designed the study; Y.Z., X.Z., and Q.G. prepared the figures. Y. Li wrote the main manuscript text, and all authors reviewed the manuscript.

ACKNOWLEDGMENTS

This work was supported by the National Natural Science Foundation of China (81672776 and 81200975 to Y. Li, 31501838 to X.Z.). The authors thank Dr. John M. Szymanski for help with the preparation of the manuscript.

Received: November 12, 2016
Revised: July 3, 2017
Accepted: July 4, 2017
Published: August 8, 2017

REFERENCES

Bass, A.J., Watanabe, H., Mermel, C.H., Yu, S., Perner, S., Verhaak, R.G., Kim, S.Y., Wardwell, L., Tamayo, P., Gat-Viks, I., et al. (2009). SOX2 is an amplified lineage-survival oncogene in lung and esophageal squamous cell carcinomas. Nat. Genet. *41*, 1238–1242.

Beck, B., and Blanpain, C. (2013). Unravelling cancer stem cell potential. Nat. Rev. Cancer *13*, 727–738.

Bora-Singhal, N., Perumal, D., Nguyen, J., and Chellappan, S. (2015). Gli1-mediated regulation of sox2 facilitates self-renewal of stem-like cells and confers resistance to egfr inhibitors in non-small cell lung cancer. Neoplasia *17*, 538–551.

Boumahdi, S., Driessens, G., Lapouge, G., Rorive, S., Nassar, D., Le Mercier, M., Delatte, B., Caauwe, A., Lenglez, S., Nkusi, E., et al. (2014). SOX2 controls tumour initiation and cancer stem-cell functions in squamous-cell carcinoma. Nature *511*, 246–250.

Bouzas, S.O., Marini, M.S., Torres Zelada, E., Buzzi, A.L., Morales Vicente, D.A., and Strobl-Mazzulla, P.H. (2016). Epigenetic activation of Sox2 gene in the developing vertebrate neural plate. Mol. Biol. Cell *27*, 1921–1927.

Chan, K.S., Espinosa, I., Chao, M., Wong, D., Ailles, L., Diehn, M., Gill, H., Presti, J., Jr., Chang, H.Y., van de Rijn, M., et al. (2009). Identification, molecular characterization, clinical prognosis, and therapeutic targeting of human bladder tumor-initiating cells. Proc. Natl. Acad. Sci. USA *106*, 14016–14021.

Chan, K.S., Volkmer, J.P., and Weissman, I. (2010). Cancer stem cells in bladder cancer: a revisited and evolving concept. Curr. Opin. Urol. *20*, 393–397.

Favaro, R., Valotta, M., Ferri, A.L., Latorre, E., Mariani, J., Giachino, C., Lancini, C., Tosetti, V., Ottolenghi, S., Taylor, V., et al. (2009). Hippocampal development and neural stem cell maintenance require Sox2-dependent regulation of Shh. Nat. Neurosci. *12*, 1248–1256.

Ferone, G., Song, J.Y., Sutherland, K.D., Bhaskaran, R., Monkhorst, K., Lambooij, J.P., Proost, N., Gargiulo, G., and Berns, A. (2016). SOX2 is the determining oncogenic switch in promoting lung squamous cell carcinoma from different cells of origin. Cancer Cell *30*, 519–532.

Foshay, K.M., and Gallicano, G.I. (2008). Regulation of Sox2 by STAT3 initiates commitment to the neural precursor cell fate. Stem Cells Dev. *17*, 269–278.

Hatina, J., and Schulz, W.A. (2012). Stem cells in the biology of normal urothelium and urothelial carcinoma. Neoplasma *59*, 728–736.

Ho, P.L., Kurtova, A., and Chan, K.S. (2012a). Normal and neoplastic urothelial stem cells: getting to the root of the problem. Nat. Rev. Urol. *9*, 583–594.

Ho, P.L., Lay, E.J., Jian, W., Parra, D., and Chan, K.S. (2012b). Stat3 activation in urothelial stem cells leads to direct progression to invasive bladder cancer. Cancer Res. *72*, 3135–3142.

Hutz, K., Mejias-Luque, R., Farsakova, K., Ogris, M., Krebs, S., Anton, M., Vieth, M., Schuller, U., Schneider, M.R., Blum, H., et al. (2014). The stem cell factor SOX2 regulates the tumorigenic potential in human gastric cancer cells. Carcinogenesis *35*, 942–950.

Islam, S.S., Mokhtari, R.B., Noman, A.S., Uddin, M., Rahman, M.Z., Azadi, M.A., Zlotta, A., van der Kwast, T., Yeger, H., and Farhat, W.A. (2016). Sonic hedgehog (Shh) signaling promotes tumorigenicity and stemness via activation of epithelial-to-mesenchymal transition (EMT) in bladder cancer. Mol. Carcinog. *55*, 537–551.

Kitamura, H., Torigoe, T., Hirohashi, Y., Asanuma, H., Inoue, R., Nishida, S., Tanaka, T., Fukuta, F., Masumori, N., Sato, N., et al. (2013). Prognostic impact of the expression of ALDH1 and SOX2 in urothelial cancer of the upper urinary tract. Mod. Pathol. *26*, 117–124.

Kogure, M., Takawa, M., Cho, H.S., Toyokawa, G., Hayashi, K., Tsunoda, T., Kobayashi, T., Daigo, Y., Sugiyama, M., Atomi, Y., et al. (2013). Deregulation of the histone demethylase JMJD2A is involved in human carcinogenesis through regulation of the G(1)/S transition. Cancer Lett. *336*, 76–84.

Leis, O., Eguiara, A., Lopez-Arribillaga, E., Alberdi, M.J., Hernandez-Garcia, S., Elorriaga, K., Pandiella, A., Rezola, R., and Martin, A.G. (2012). Sox2 expression in breast tumours and activation in breast cancer stem cells. Oncogene *31*, 1354–1365.

Liu, K., Jiang, M., Lu, Y., Chen, H., Sun, J., Wu, S., Ku, W.Y., Nakagawa, H., Kita, Y., Natsugoe, S., et al. (2013). Sox2 cooperates with inflammation-mediated Stat3 activation in the malignant transformation of foregut basal progenitor cells. Cell Stem Cell *12*, 304–315.

Lundberg, I.V., Edin, S., Eklof, V., Oberg, A., Palmqvist, R., and Wikberg, M.L. (2016). SOX2 expression is associated with a cancer stem cell state and down-regulation of CDX2 in colorectal cancer. BMC Cancer *16*, 471.

Papafotiou, G., Paraskevopoulou, V., Vasilaki, E., Kanaki, Z., Paschalidis, N., and Klinakis, A. (2016). KRT14 marks a subpopulation of bladder basal cells with pivotal role in regeneration and tumorigenesis. Nat. Commun. *7*, 11914.

Ruan, J., Wei, B., Xu, Z., Yang, S., Zhou, Y., Yu, M., Liang, J., Jin, K., Huang, X., Lu, P., et al. (2013). Predictive value of Sox2 expression in transurethral resection specimens in patients with T1 bladder cancer. Med. Oncol. *30*, 445.

Santini, R., Pietrobono, S., Pandolfi, S., Montagnani, V., D'Amico, M., Penachioni, J.Y., Vinci, M.C., Borgognoni, L., and Stecca, B. (2014). SOX2 regulates self-renewal and tumorigenicity of human melanoma-initiating cells. Oncogene *33*, 4697–4708.

Sarkar, A., and Hochedlinger, K. (2013). The sox family of transcription factors: versatile regulators of stem and progenitor cell fate. Cell Stem Cell *12*, 15–30.

Shin, K., Lim, A., Odegaard, J.I., Honeycutt, J.D., Kawano, S., Hsieh, M.H., and Beachy, P.A. (2014). Cellular origin of bladder neoplasia and tissue dynamics of its progression to invasive carcinoma. Nat. Cell Biol. *16*, 469–478.

Torre, L.A., Bray, F., Siegel, R.L., Ferlay, J., Lortet-Tieulent, J., and Jemal, A. (2015). Global cancer statistics, 2012. CA Cancer J. Clin. *65*, 87–108.

Van Batavia, J., Yamany, T., Molotkov, A., Dan, H., Mansukhani, M., Batourina, E., Schneider, K., Oyon, D., Dunlop, M., Wu, X.R., et al. (2014). Bladder cancers arise from distinct urothelial sub-populations. Nat. Cell Biol. *16*, 982–991, 981-985.

Vanner, R.J., Remke, M., Gallo, M., Selvadurai, H.J., Coutinho, F., Lee, L., Kushida, M., Head, R., Morrissy, S., Zhu, X., et al. (2014). Quiescent sox2(+) cells drive hierarchical growth and relapse in sonic hedgehog subgroup medulloblastoma. Cancer Cell *26*, 33–47.

Williams, P.D., Lee, J.K., and Theodorescu, D. (2008). Molecular credentialing of rodent bladder carcinogenesis models. Neoplasia *10*, 838–846.

Yu, H., Kortylewski, M., and Pardoll, D. (2007). Crosstalk between cancer and immune cells: role of STAT3 in the tumour microenvironment. Nat. Rev. Immunol. *7*, 41–51.

Stem Cell Reports, Volume *9*

Supplemental Information

SOX2 Is a Marker for Stem-like Tumor Cells in Bladder Cancer

Fengyu Zhu, Weiqing Qian, Haojie Zhang, Yu Liang, Mingqing Wu, Yingyin Zhang, Xiuhong Zhang, Qian Gao, and Yang Li

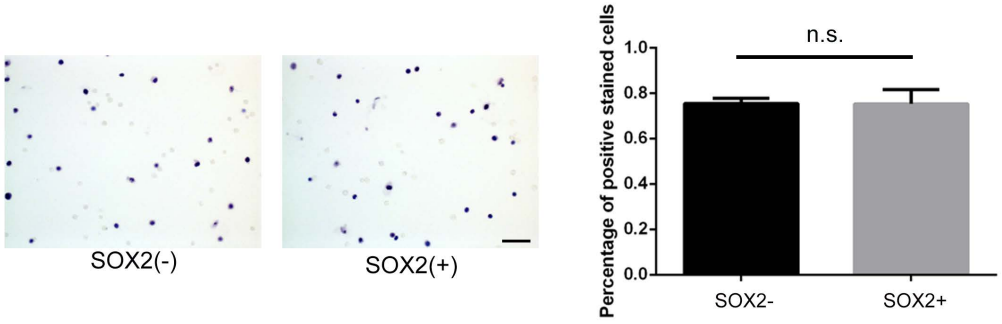

Figure S1 related to Figure 2. Validation of the cell viability after sorting. SOX2+/- cells were stained by typan blue after sorting and percentage of positive stained cells were calculated by counting 500 cells from randomly selected fields of each group, respectively. n.s.: no significant difference. Scale bars, 50 μm. Error bars represent the S.D. of three independent experiments.

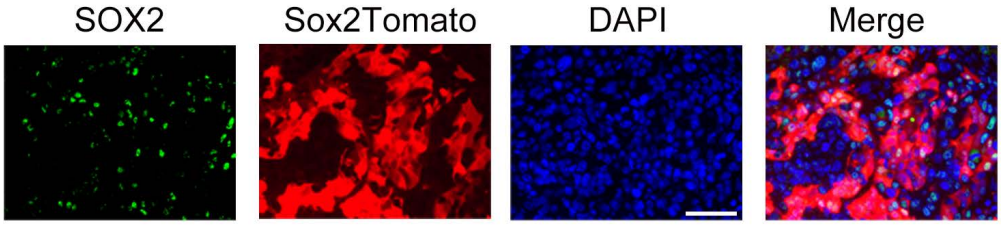

Supplementary Figure S2, related to Figure 3, Immunofluorescent staining of SOX2 after tracing. Representative image shows immunostaining by SOX2 antibodies after tracing period. Scale bars, 50 μm.

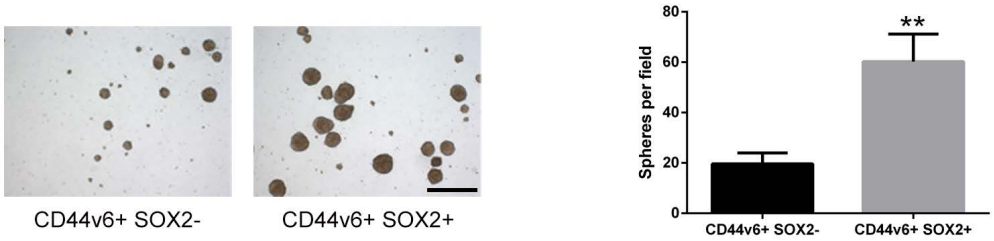

Supplementary Figure S3, related to Figure 3, Sphere formation of CD44v6+Tomato+(SOX2+) and CD44v6+Tomato-(SOX2-) cells. CD44V6+Tom+(SOX2+) and CD44V6+Tom-(SOX2-) cells were FACS sorted and cultured in stem cell medium. Cultures at 10 days are shown and the sphere numbers are plotted. **, $p<0.01$, student t-test. Scale bars, 250 μm. Error bars represent the S.D. of three independent experiments.

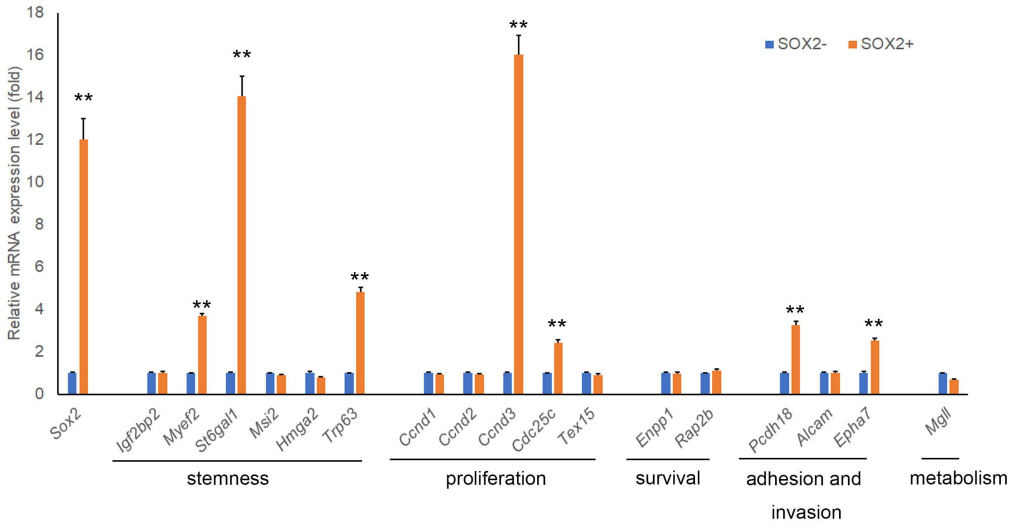

Supplementary Figure S4, related to Figure 3, Expression pattern of SOX2 target genes. CD44v6+Tomato+(SOX2+) and CD44v6+Tomato-(SOX2-) cells were sorted by FACS, and mRNA level of SOX2 target genes were examined by quantitative RT-PCR. **, $p<0.01$, student t-test. Error bars represent the S.D. of three independent experiments.

Supplemental Experimental Procedures

Mice model

Sox2-Cre^{ERT2}, *R26*^{tdTomato} and *ROSA-DT*A mice were obtained from Jackson Laboratory. BBN(sc-486264, Santa Cruz) was dissolved in drinking water at a concentration of 0.05% (w/v) and provided to transgenic male mice for indicated times as previous described(Shin et al., 2014). Tamoxifen (T5648) were purchased from Sigma. For transplantation assays into immunodeficient mice, the different FACS-isolated cell populations (Sox2 Tomato+/-) from BBN-induced mice BCa tissue were collected in 4 ℃ medium. For limited dilution assay, different dilutions (64,000/16,000/4,000/1,000) of cells resuspended in 50 μl of Matrigel (Corning, 354230) were injected subcutaneously into BALB/cASlac-nu nude mice (Shanghai Laboratory Animals Center, SLAC). Secondary tumors were monitored weekly until mice presented signs of distress, and the mice were sacrificed. All animal procedures were performed under a protocol approved by the Laboratory Animal Center of Anhui Medical University and in accordance with National Institutes of Health guide for the care and use of Laboratory animals (NIH Publications No. 8023, revised 1978).

Clinical sample

22 human BCa samples were obtained from Department of Urology, Huadong Hospital, Fudan University with patients' informed consent. The pathological condition of the BPH samples was determined by experienced urologists at Huadong Hospital.

Immunostaining

For frozen section, tissues were fixed in 4% paraformaldehyde at 4 ℃ for 48 h, followed with placing into 30% sucrose overnight and frozen in optimal cutting temperature (OCT) compound (Tissue Tek, Sakura). Frozen 10 mm sections were obtained and processed as previously described. For paraffin sections of bladder cancer tissue samples from mice and human patient were antigen retrieved, blocked and processed as described before(Liu et al., 2016). Hematoxylin–eosin stains were performed using standard histology procedures. The intensity of immunostaining was measured by Image-Pro Plus 6.0 image analysis software (Media Cybernetics). The intensity of each image was calculated by normalizing the average integrated optical density (IOD) with the total selected area of interest (AOI).

Primary antibodies					
Protein target	Company	Catalog Number	Host species	Clonality	Dilution
SOX2	Abcam	ab97959	Rabbit	polyclonal	1:100
KRT14	ProteinTech	60320-1-Ig	Mouse	monoclonal	1:150
Human CD44v6	Abcam	ab78960	Mouse	monoclonal	1:150
Mouse CD44v6	Thermo Fisher	33-6700	Mouse	monoclonal	1:150
Ki67	Thermo Fisher	PA5-19462	Rabbit	polyclonal	1:200
LAMININ	Abcam	ab11575	Rabbit	polyclonal	1:200
UroplakinIII	Abcam	ab78196	Mouse	monoclonal	1:200
Phospho-Stat3	Cell signaling	#9134	Rabbit	polyclonal	1:150

CD3	Abgent	AP52283	Rabbit	polyclonal	1:150
Secondary antibodies					
FITC conjugate	Proteintech	SA00003-2	Goat anti-rabbit IgG		1:200
FITC conjugate	Proteintech	SA00003-1	Goat anti-mouse IgG		1:200
TRITC conjugate	Proteintech	SA00007-2	Goat anti-rabbit IgG		1:200

FACS isolation and acquisition

Tumours were digested and blocked as previously described(Boumahdi et al., 2014). Immunostaining was performed using APC-conjugated anti-CD44v6 (1:100, BDPharmingen, 559250) by incubation for 30 min at room temperature. Cells were selected based on the expression of Sox2-tdTomato(PE) and/or CD44v6(APC). Gates for fluorescence fractionations were established using unstained and isotype controls. FACS analysis was performed using FACSAria and FACSDiva software (BD Biosciences). Sorted cells were collected either in culture medium for *in vivo* transplantation experiments or into lysis buffer for RNA extraction.

Sphere formation

FACS-sorted cells were cultured in ultra-low attachment plates (Corning Inc., Corning, NY, USA) at a density of 1,000 cells per well. Cells were cultured in modified serum-free culture mediums reported previously(Zhu et al., 2013). Spheres with a diameter over 20 μm were counted 3 days after plating.

Examine of gene expression level

Bladder samples were snap frozen in liquid nitrogen, homogenized with a mortar and pestle, and RNA extracted with the TRIzol (Invitrogen). Quantitative RT-PCR and western blot was performed as previously described(Li et al., 2015; Li et al., 2011). The primers used for RT-PCR is listed below.

Primer Names	Sequence
Sox2 F	5’-ACAGATGCAACCGATGCACC-3’
Sox2 R	5’-TGGAGTTGTACTGCAGGGCG-3
CD44v6 F	5'- CCTTGGCCACCACTCCTAATAG -3'
CD44v6 R	5'- CAGTTGTCCCTTCTGTCACATG -3'
Krt14 F	5'- AGCGGCAAGAGTGAGATTTCT -3'
Krt14 R	5'- CCTCCAGGTTATTCTCCAGGG -3'
Igf2bp2 F	5'- GTCCTACTCAAGTCCGGCTAC-3'
Igf2bp2 R	5'- CATATTCAGCCAACAGCCCAT-3'
Myef2 F	5'- GGGTCCAAGTGGAGTTGGG-3'
Myef2 R	5'- GCACTGCCAAGTCTACCAAAG-3'
St6gal1 F	5'- CTCCTGTTTGCCATCATCTGC-3'
St6gal1 R	5'- GGGTCTTGTTTGCTGTTTGAGA-3'
Msi2 F	5'- CTACAGTGCTCAACCGAATTTTG-3'
Msi2 R	5'- CTGGCCGCGCTTATGTAAT-3'
Hmga2 F	5'- GAGCCCTCTCCTAAGAGACCC-3'

Hmga2 R	5'- TTGGCCGTTTTTCTCCAATGG-3'
Trp63 F	5'- TACTGCCCCGACCCTTACAT-3'
Trp63 R	5'- GCTGAGGAACTCGCTTGTCTG-3'
Ccnd1 F	5'- GCGTACCCTGACACCAATCTC-3'
Ccnd1 R	5'- CTCCTCTTCGCACTTCTGCTC-3'
Ccnd2 F	5'- GAGTGGGAACTGGTAGTGTTG-3'
Ccnd2 R	5'- CGCACAGAGCGATGAAGGT-3'
Ccnd3 F	5'- CGAGCCTCCTACTTCCAGTG-3'
Ccnd3 R	5'- GGACAGGTAGCGATCCAGGT-3'
Cdc25c F	5'- AAAATGCAGCGTTCCTGCTTC-3'
Cdc25c R	5'- CTTGGGGTCCTAGTGCCTC-3'
Tex15 F	5'- TCATACCCACTGGTAACACAGC-3'
Tex15 R	5'- GGCAAAACATCACTCAAACCTG-3'
Enpp1 F	5'- CTGGTTTTGTCAGTATGTGTGCT-3'
Enpp1 R	5'- CTCACCGCACCTGAATTTGTT-3'
Rap2b F	5'- GCTCACCGTGCAGTTCGTAA-3'
Rap2b R	5'- GCTGTAGACGAGAATGAAGCC-3'
Pcdh18 F	5'- ATGCACTTTAGATTTGCACTTGC-3'
Pcdh18 R	5'- CAATTACCGATCCGACCCTCT-3'
Alcam F	5'- GGCAGTGGGTTCGTCATAAAC-3'
Alcam R	5'- ATCGCAGAGACATTCAGGGAG-3'
Epha7 F	5'- TGACCCTGAAACCTATGAGGAC-3'
Epha7 R	5'- ATTCTCCTGCACCAATCACAC-3'
Mgll F	5'-ACCATGCTGTGATGCTCTCTG-3'
Mgll R	5'-CAAACGCCTCGGGGATAACC-3'
Gapdh F	5'- AGGTCGGTGTGAACGGATTTG -3'
Gapdh R	5'- GGGGTCGTTGATGGCAACA -3'

Invasion assay

BioCoat™ Matrigel invasion chamber was used according to the manufacturer's instruction (BD Biosciences). Briefly, 4×10^4 isolated cells by the flow cytometry were resuspended in 100 μl of DMEM medium, and seeded in the upper portion of the invasion chamber. The lower portion of the chamber contained 500 μl of medium supplemented with 2% FBS and glutamine, which served as a chemoattractant. After 36 h, non-invasive cells were removed from the upper surface of the membrane with a cotton swab. The invasive cells on the lower surface of the membrane were stained with crystal violet, and counted in four separate areas with an inverted microscope(Chen et al., 2011).

Statistics

Data are presented as the means±standard deviation (S.D.) or standard error (S.E.). All of the statistical analyses were performed using Excel (Microsoft, Redmond, WA) or Prism (GraphPad Software Inc., La Jolla, CA). The two-tailed Student's t-test or one way ANOVA were used and a P-value of <0.05 was considered significant.

Supplemental References

Boumahdi, S., Driessens, G., Lapouge, G., Rorive, S., Nassar, D., Le Mercier, M., Delatte, B., Caauwe, A., Lenglez, S., Nkusi, E*., et al.* (2014). SOX2 controls tumour initiation and cancer stem-cell functions in squamous-cell carcinoma. Nature *511*, 246-250.

Chen, Y., Wang, D., Guo, Z., Zhao, J., Wu, B., Deng, H., Zhou, T., Xiang, H., Gao, F., and Yu, X. (2011). Rho kinase phosphorylation promotes ezrin-mediated metastasis in hepatocellular carcinoma. Cancer research *71*, 1721-1729.

Li, Y., Deng, H., Lv, L., Zhang, C., Qian, L., Xiao, J., Zhao, W., Liu, Q., Zhang, D., Wang, Y*., et al.* (2015). The miR-193a-3p-regulated ING5 gene activates the DNA damage response pathway and inhibits multi-chemoresistance in bladder cancer. Oncotarget *6*, 10195-10206.

Li, Y., Yu, Y., Zhang, Y., Zhou, Y., Li, C., Zhu, J., Yuan, H., and Lu, H. (2011). MAFIP is a tumor suppressor in cervical cancer that inhibits activation of the nuclear factor-kappa B pathway. Cancer Sci *102*, 2043-2050.

Liu, W., Zhou, L., Zhou, C., Zhang, S., Jing, J., Xie, L., Sun, N., Duan, X., Jing, W., Liang, X*., et al.* (2016). GDF11 decreases bone mass by stimulating osteoclastogenesis and inhibiting osteoblast differentiation. Nature communications *7*, 12794.

Shin, K., Lim, A., Zhao, C., Sahoo, D., Pan, Y., Spiekerkoetter, E., Liao, J.C., and Beachy, P.A. (2014). Hedgehog signaling restrains bladder cancer progression by eliciting stromal production of urothelial differentiation factors. Cancer cell *26*, 521-533.

Zhu, Y.T., Lei, C.Y., Luo, Y., Liu, N., He, C.W., Chen, W., Li, F., Deng, Y.J., and Tan, W.L. (2013). A modified method for isolation of bladder cancer stem cells from a MB49 murine cell line. BMC urology *13*, 57.